

Figure 5. Excitation profiles of $\nu(\text{O}_2)$ and $\nu_s(\text{CoO})$ of $[\text{Co}(\text{salen})]_2\text{O}_2$: ●, $\nu(\text{O}_2)$ at 1011 cm^{-1} ; ▲, $\nu_s(\text{CoO})$ at 533 cm^{-1} .

$d-\pi^*$ transitions of $\text{Co}(\text{salen})$, $d-d$ transitions of the Co atom, and $\text{Co}-\text{O}_2$ CT transitions of the $\text{Co}-\text{O}_2$ moiety although such classifications are valid only for ideal cases where the mixing of these orbitals are minimal. However, they are sufficient for our qualitative discussion of the electronic transitions involved.

The electronic spectrum of crystalline $[\text{Co}(\text{salen})]_2\text{O}_2$ yielded only a broad band in the 340–740-nm region without

any distinct maxima. Thus, it was almost impossible to obtain information about the individual transitions. In such cases, excitation profile studies of RR spectra have proved to be very useful in locating individual electronic transitions.²⁸ Previously, we⁷ have located the $\text{Co}-\text{O}_2$ CT transitions of the $[\text{Co}(\text{salen})\text{B}]_2\text{O}_2$ -type compounds at ca. 500 nm on the basis of the excitation profiles of their $\nu(\text{O}_2)$ and $\nu(\text{CoO})$.

Figure 5 shows the excitation profiles of the $\nu(\text{O}_2)$ (1011 cm^{-1}) and $\nu_s(\text{CoO})$ (533 cm^{-1}) of $[\text{Co}(\text{salen})]_2\text{O}_2$. The $\nu(\text{O}_2)$ shows a single maximum near 570 nm, indicating the presence of a $\text{Co}-\text{O}_2$ CT band near 570 nm. As discussed in our previous paper,⁷ this is a transition from the $\alpha d_{z^2} + \beta \pi^*(\text{O}_2)$ to the $\beta d_{z^2} - \alpha \pi^*(\text{O}_2)$ orbital ($\beta > \alpha$). If the energy gap between these two orbitals is largely determined by the energies of their original orbitals,⁷ the red shift of the $\text{Co}-\text{O}_2$ CT band in going from $[\text{Co}(\text{salen})\text{B}]_2\text{O}_2$ to $[\text{Co}(\text{salen})]_2\text{O}_2$ is understandable since the absence of a base ligand lowers the d_{z^2} orbital. The excitation profile of the $\nu_s(\text{CoO})$ exhibits two maxima at ca. 570 and 500 nm. The presence of the maximum at 570 nm is expected since this vibration should be resonance enhanced by the $\text{Co}-\text{O}_2$ CT transition. The presence of the second maximum near 500 nm may indicate that the $d-\pi^*$ transition of $\text{Co}(\text{salen})$ is in this vicinity.

Acknowledgment. This work was supported by the National Science Foundation (Grant No. CHE-7915169). We thank Professor D. P. Strommen of Carthage College for helpful discussions.

Registry No. $[\text{Co}(\text{salen})]_2\text{O}_2$, 23602-28-0; $\text{Co}(\text{salen})$, 14167-18-1; ^{18}O , 14797-71-8.

(28) D. L. Jeanmaire and R. P. Van Duyne, *J. Am. Chem. Soc.*, **98**, 4034 (1976).

Contribution from the Department of Chemistry and Biochemistry, Utah State University, Logan, Utah 84322, and Fakultät für Biologie, Universität Konstanz, D-7750 Konstanz, Germany

Tungsten(V)-Oxo and Tungsten(VI)-Dioxo Complexes with Oxygen, Nitrogen, and Sulfur Ligands. Electrochemical, Infrared, and Electron Paramagnetic Resonance Studies

C. A. RICE,^{1a} P. M. H. KRONECK,^{1b} and J. T. SPENCE*^{1a}

Received September 19, 1980

Six new tungsten(V)- and -(VI)-oxo complexes have been synthesized (WOCl_3L , $\text{L} = \alpha, \alpha'$ -bipyridyl and *o*-phenanthroline; WOCIL_2 , WO_2L_2 , $\text{L} = 8$ -hydroxyquinoline and 8-mercaptoquinoline) and their electrochemical properties, IR spectra, and EPR parameters determined. In addition, EPR and electrochemical data for five previously reported tungsten-oxo complexes ($\text{WOCl}_3(\text{bpy})$; $\text{WO}_2\text{X}_2\text{L}$, $\text{X} = \text{Cl}, \text{Br}$, $\text{L} = \alpha, \alpha'$ -bipyridyl, *o*-phenanthroline; $\text{WO}_2(\text{aac})_2$) have also been obtained. Cyclic voltammograms of both tungsten(V) and -(VI) complexes show reduction peaks that are considerably more negative than those of the corresponding molybdenum complexes, and the reductions are less reversible. The tungsten(V) EPR signals are much broader and the g values are significantly lower than those of molybdenum(V) complexes. The results support the hypothesis that tungsten occupies the same binding site as molybdenum when substituted in the enzyme sulfite oxidase, with the lack of catalytic activity of the tungsten enzyme attributed to the lower reduction potential of tungsten as compared with that of molybdenum.

Among the elements of subgroup 6, chromium, molybdenum, and tungsten, only molybdenum has attracted great interest over the past two decades due to its important catalytic versatility in the fields of chemistry and biology. Recently tungsten has been incorporated into several molybdenum en-

zymes such as nitrogenase,² nitrate reductase,³ and sulfite oxidase.⁴ It substitutes for molybdenum, producing cata-

(2) J. R. Benneman, G. M. Smith, P. J. Kostel, and C. E. McKenna, *FEBS Lett.*, **29**, 219 (1973).

(3) E. J. Hewitt and B. A. Notton in "Molybdenum and Molybdenum Containing Enzymes", M. P. Coughlan, Ed., Pergamon Press, Elmsford, NY, 1980, p 273.

(1) (a) Utah State University. (b) Universität Konstanz.

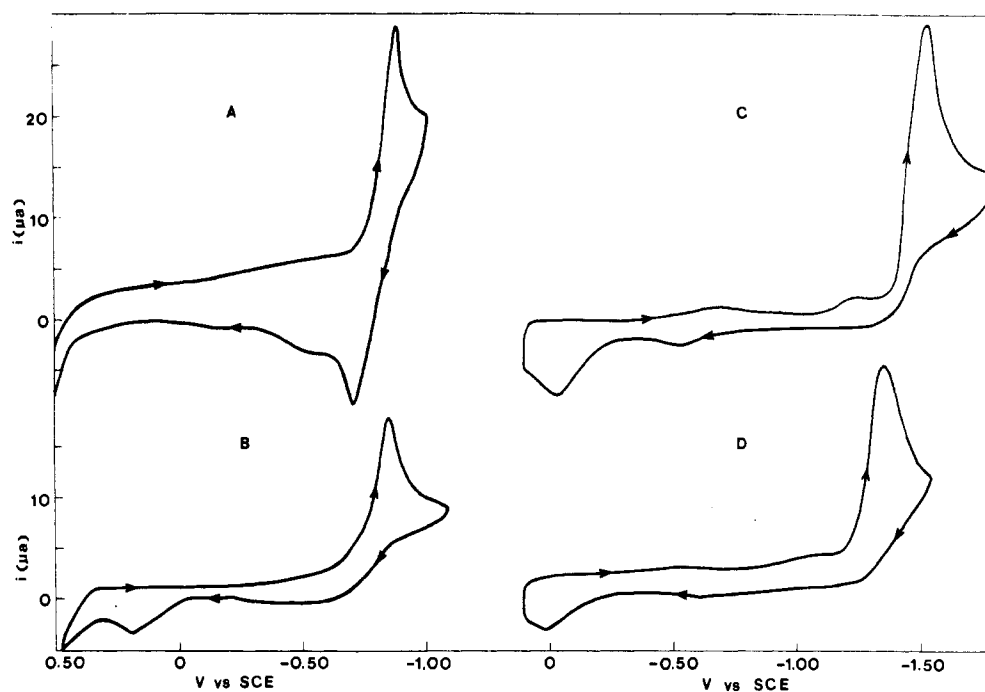


Figure 1. Cyclic voltammograms (5×10^{-4} M, in DMF, 0.10 M $(C_2H_5)_4NCl$): A, *cis*- $WOCl(ox)_2$; B, *cis*- $WOCl(tox)_2$; C, $WO_2(ox)_2$; D, $WO_2(tox)_2$.

lytically inactive tungsten enzymes with the hexavalent metal most likely bound at the active site. In the case of tungsten sulfite oxidase,⁴ the metal can be reduced to the tungsten(V) state by substrate-reduced residual molybdenum centers in the preparation.⁴ Thus, tungsten may develop into a useful probe for the active site of molybdenum enzymes, giving further structural information about the ligands involved in molybdenum binding. Recent evidence indicates formate dehydrogenase from *Clostridium* species may require, besides selenium, tungsten either by itself or in combination with molybdenum, for catalytic activity.⁵ The properties of model tungsten complexes are therefore of considerable interest, for understanding both the possible biological function of the metal and, by comparison with properties of the molybdenum analogues, the biological differences between the two metals. Earlier investigations by Callis and Wentworth⁶ on the reactions of MoO_4^{2-} or WO_4^{2-} with methyliminodiacetic acid and L-cysteine have shown that the formation constants for both complexes are very similar. On the other hand, molybdenum is reduced much more easily in the physiological range of pH than tungsten.

We report here the synthesis of six new tungsten-oxo complexes and a study of their electrochemical, infrared, and electron paramagnetic resonance (EPR) properties. In addition, the electrochemical, infrared, and EPR properties of five known tungsten-oxo complexes have also been determined. The tungsten(V)-oxo complexes have the formula $WOCl_3L$, $L = \alpha, \alpha'$ -bipyridine and *o*-phenanthroline, or $WOCIL_2$, $L = 8$ -hydroxyquinoline and 8-mercaptoquinoline; the tungsten(VI)-dioxo complexes have the formula WO_2L_2 , $L =$ acetylacetonate, 8-hydroxyquinoline, and 8-mercaptoquinoline, or WO_2X_2L , $X =$ chlorine or bromine, $L = \alpha, \alpha'$ -bipyridine and *o*-phenanthroline. The results are compared to the electrochemical and EPR properties of the corresponding molybde-

Table I. Electrochemical Properties of Oxotungsten(V) and Dioxotungsten(VI) Complexes^a

complex	E_{pc}^b	E_{pa}^c	ΔE_p^d	n^e
<i>cis</i> - $WOCl_3(bpy)$ (green)	-0.61	-0.47	0.14	0.98
<i>trans</i> - $WOCl_3(bpy)$ (purple)	-0.58	-0.51	0.07	0.96
<i>trans</i> - $WOCl_3(phen)$	-0.64	-0.50	0.14	1.01
<i>cis</i> - $WOCl(ox)_2$	-0.87	-0.70	0.17	0.82
<i>cis</i> - $WOCl(tox)_2$	-0.85	+0.18	1.03	0.93
$WO_2Cl_2(bpy)$	-1.25	-0.95	0.30	
$WO_2Cl_2(phen)$	-1.23	-0.94	0.29	
$WO_2(ox)_2$	-1.51	-0.04	1.47	
$WO_2(tox)_2$	-1.34	-0.00	1.34	
$WO_2Br_2(bpy)$	<i>f</i>			
$WO_2(acac)_2$	<i>f</i>			

^a 5.00×10^{-4} M in DMF, 0.10 M $(C_2H_5)_4NCl$, scan rate 0.100 V s^{-1} . ^b Reduction peak, ± 0.01 V vs. SCE. ^c Oxidation peak, ± 0.01 V vs. SCE. ^d Difference between E_{pc} and E_{pa} , V. ^e $n =$ number of electrons per molecule. Coulometric reduction, average of two or more results, ± 0.05 . ^f Unstable in DMF.

num(VI)-dioxo and molybdenum(V)-oxo complexes reported recently.^{8,9}

Results

Electrochemistry. The electrochemical properties of tungsten(VI)-dioxo and tungsten(V)-oxo complexes are similar to those of the corresponding molybdenum complexes.⁸ The tungsten(V) complexes are readily reduced in a one-electron step at a platinum cathode in dimethylformamide (DMF) to tungsten(IV) species, but they are not oxidizable to the corresponding tungsten(VI)-dioxo complexes under the conditions used, results also observed with molybdenum(V) complexes.⁸ Major differences between the two metals are found, however, in the cyclic voltammetric peak potentials and the degree of reversibility of the reductions. The tungsten complexes have reduction peaks 0.30–0.50 V more negative than those of the molybdenum complexes, and the reductions are less reversible (Table I, Figure 1).

(4) J. L. Johnson and K. V. Rajagopalan, *J. Biol. Chem.*, **251**, 5505 (1976).

(5) L. G. Ljungdahl in "Molybdenum and Molybdenum Containing Enzymes", M. P. Coughlan, Ed., Pergamon Press, Elmsford, NY, 1980, p 463.

(6) G. E. Callis and R. A. D. Wentworth, *Bioinorg. Chem.*, **7**, 57 (1977).

(7) Ligand abbreviations: bpy = α, α' -bipyridyl; phen = *o*-phenanthroline; ox = 8-hydroxyquinoline; tox = 8-mercaptoquinoline; acac = acetylacetonate.

(8) R. D. Taylor, J. P. Street, M. Minelli, and J. T. Spence, *Inorg. Chem.*, **17**, 3207 (1978).

(9) M. I. Scullane, R. D. Taylor, M. Minelli, J. T. Spence, K. Yamanouchi, J. H. Enemark, and N. D. Chasteen, *Inorg. Chem.*, **18**, 3213 (1979).

Table II. EPR Parameters of Tungsten and Molybdenum Complexes^a

complex	metal (color)	$\langle g_0 \rangle$	g_1	g_2	g_3	ref
MOCl ₅ ²⁻	Mo (green)	1.946	1.970	1.938	1.938	9
	W (green)	1.773	1.804	1.758	1.758	11
<i>cis</i> -MOCl ₃ (bpy)	Mo (green)	1.952	1.968	1.953	1.938	9
	W (green)	1.795	1.844	1.775	1.775	
<i>trans</i> -MOCl ₃ (bpy)	Mo (red)	1.948	1.971	1.944	1.931	9
	W (purple)	1.794	1.844	1.774	1.774	
<i>trans</i> -MOCl ₃ (phen)	Mo (red)	1.947	1.971	1.941	1.929	9
	W (blue)	1.792	1.795	1.771	1.771	
<i>cis</i> -WOCl(ox) ₂	Mo (green)	1.954	1.970	1.953	1.939	9
	W (green)	1.835	1.886	1.835	1.793	
<i>cis</i> -WOCl(tox) ₂	Mo (black)	1.967	2.003	1.952	1.948	9
	W (red)	1.862	1.940	1.831	1.831	
sulfite oxidase	Mo	1.9805	2.0037	1.9720	1.9658	<i>b</i>
	W	1.910	1.982	1.889	1.889	4

^a 120 K, $\sim 5 \times 10^{-4}$ M in DMF, 0.1 M (C₂H₅)₄NCl. ^b M. T. Lamy, S. Gutteridge, and R. C. Bray, *Biochem. J.*, 185, 397 (1980). $\langle g_0 \rangle$ in the case of sulfite oxidase is the calculated value from anisotropic g values.

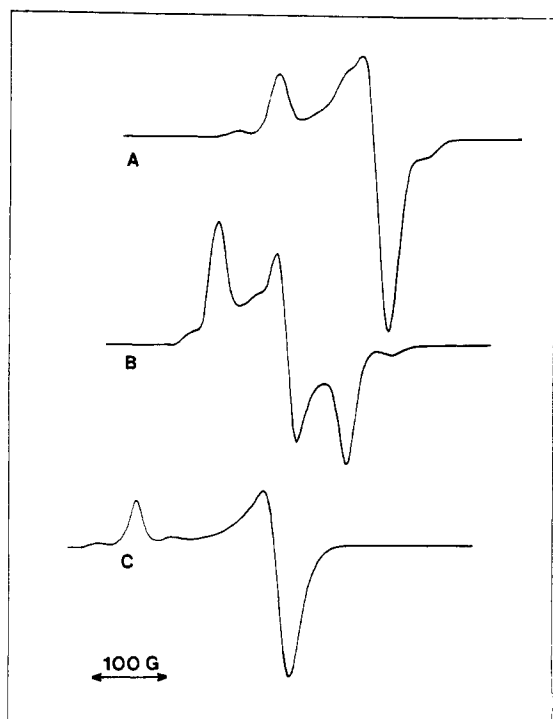


Figure 2. X-Band EPR spectra of tungsten(V)-oxo complexes (120 K, $\sim 5 \times 10^{-4}$ M in DMF, 0.10 M (C₂H₅)₄NCl): A, *trans*-WOCl₃(bpy); B, *cis*-WOCl(ox)₂; C, *cis*-WOCl(tox)₂.

Similar differences are observed for the peak potentials and reversibility of reduction of the tungsten(VI)-dioxo complexes in comparison with the corresponding molybdenum(VI)-dioxo complexes (Table I, Figure 1). As with the molybdenum(VI) compounds, attempts to determine the number of electrons involved in reduction of the tungsten(VI) complexes by controlled-potential coulometry were unsuccessful due to high residual currents indicative of secondary processes.⁸ Isbell and Sawyer reported similar results with MoO₂(ox)₂ and concluded either an oxo-bridged molybdenum(V) dimer or molybdenum(IV) complex is formed upon reduction.¹⁰

EPR Spectra at X-Band. The EPR parameters for the tungsten(V)-oxo complexes are compiled in Table II. Figure 2 illustrates representative spectra of the complexes WOCl₃L and WOClL₂ measured in frozen solution at 120 K. For comparison EPR parameters of the corresponding molybdenum(V)-oxo analogues and both molybdenum(V) and tungsten(V) sulfite oxidase are given. Generally, the spectra both

Table III. Infrared Stretching Frequencies of Oxotungsten(V) and Dioxotungsten(VI) Complexes^a

complex	$\nu(\text{WO})$, cm ⁻¹	complex	$\nu(\text{WO})$, cm ⁻¹
<i>cis</i> -WOCl ₃ (bpy) (green)	970 ^b	WO ₂ Cl ₂ (phen)	943, 916 ^d
<i>trans</i> -WOCl ₃ (bpy) (purple)	952	WO ₂ Br ₂ (bpy)	954, 907 ^c
<i>trans</i> -WOCl ₃ (phen)	955	WO ₂ (ox) ₂	958, 918
<i>cis</i> -WOCl(ox) ₂	948	WO ₂ (tox) ₂	950, 910
<i>cis</i> -WOCl(tox) ₂	947	WO ₂ (acac) ₂	960, 912 ^e
WO ₂ Cl ₂ (bpy)	955, 916 ^c		

^a Solid mull. ^b Reference 15. ^c Reference 17. ^d Reference 18. ^e Reference 19.

at room temperature and 120 K are similar in shape to those of the molybdenum(V) analogues.⁹ But, as observed earlier for the pentachloro complex WOCl₅²⁻¹¹ and sulfite oxidase,⁴ the line widths of the tungsten(V)-oxo complexes and the tungsten-incorporated enzyme are significantly broader. Because of stronger spin-orbit coupling,¹² the g values are considerably lower for tungsten(V), as documented in Table II. Hyperfine splittings due to ¹⁸³W (14% natural abundance, $I = 1/2$) are obscured in all solution spectra because of the increased line width, but the expected doublet can be at least partially resolved in the low-temperature spectra in several compounds (Figure 2, b and c). Although precise A^W values were not obtained so far by computer simulation, as most recently reported for the corresponding molybdenum(V) species,⁹ the hyperfine splitting constants of the tungsten complexes are generally larger than those of corresponding molybdenum complexes. With the exception of the 8-hydroxyquinoline complex, WOCl(ox)₂, which shows a clearly resolved rhombic spectrum with three g values at X band (Figure 2b), all the other tungsten(V) compounds in Table II give an axial type EPR signal, as also observed in the case of the molybdenum(V) complexes.⁹ Substitution of the quinolinehydroxy function by a mercapto group leads to an increase of $\langle g_0 \rangle$ and of the anisotropic g values, respectively, with $\Delta g_0 = 0.027$ for tungsten vs. 0.013 for molybdenum (Table II). Similarly, the difference between g_{xx} and g_{yy} (denoted g_3 and g_2 in this paper) decreases for the 8-mercaptoquinoline complexes of both tungsten and molybdenum by comparison to their 8-hydroxyquinoline complexes (Figure 1, b and c); i.e., whereas WOCl(tox)₂ gives an axial EPR signal at approximately 9.3 GHz, the corresponding complex WOCl(ox)₂ exhibits three g values and rhombic symmetry under these conditions.

(11) H. Kon and N. E. Sharpless, *J. Phys. Chem.*, 70, 105 (1966).

(12) B. A. Goodman and J. B. Raynor, *Adv. Inorg. Chem. Radiochem.*, 13, 135 (1970).

(10) A. F. Isbell, Jr., and D. T. Sawyer, *Inorg. Chem.*, 10, 2449 (1971).

Infrared Spectra. W=O stretching bands for both tungsten(V) and -(VI) complexes are reported in Table III. Values reported in the literature have been confirmed, while those for new complexes are in the anticipated range. Dioxotungsten-(VI) complexes exhibit two bands, as expected for the *cis*-dioxo group.¹³

Discussion

As was observed with Mo(V) complexes,⁸ oxidation and reduction peak potentials differ only slightly for *cis* and *trans* isomers (WOC₃(bpy)), while substitution of sulfur for oxygen shifts the reduction potentials of both W(V) and W(VI) (WO₂(tox)₂, WOCl(tox)₂) to more positive potentials and results in a completely irreversible reduction for the W(V) complex.

While care must be exercised in drawing conclusions from irreversible or semireversible electrochemical processes, the considerably more negative (0.30–0.50 V) peak potentials of both the tungsten(VI)-dioxo and tungsten(V)-oxo complexes, as compared to the potentials of the corresponding molybdenum complexes, may account for the observed lack of activity of enzymes in which tungsten has been incorporated. In the case of sulfite oxidase, it was concluded the tungsten center is not reducible by substrate (the observed W(V) EPR signal is due to reduction of the tungsten center by substrate-reduced residual molybdenum present in the preparation; further reduction to a W(IV) state was not observed).⁴ Even in formate dehydrogenase, which appears to have a tungsten requirement, no evidence could be obtained for reduction of tungsten by substrate.⁵ The data reported here support the hypothesis that molybdenum is utilized by the enzymes in preference to tungsten for thermodynamic reasons.

At present no detailed computer analysis of the individual EPR spectra has been performed. Thus, as demonstrated by Scullane et al.,⁹ structural relationships based on spectrophotometric and EPR data can be very complicated, especially in those cases where two geometrical isomers are possible, as shown for MoOCl₃(bpy). By analogy to the data obtained for this molybdenum complex, the purple compound WOC₃(bpy) was assigned as the *trans* isomer,⁹ whereas the green complex was assigned as the *cis* isomer. Unfortunately, no crystallographic data are available for the tungsten complexes WOCl₃L, in contrast to the molybdenum analogues,⁹ which would allow a better understanding and interpretation of the EPR data. We also assume *cis* structures for both the 8-hydroxyquinoline and 8-mercaptoquinoline complexes of tungsten(V), on the basis solely of the comparison with the corresponding molybdenum(V) compounds.⁹

Experimental Section

Materials. W(CO)₆, WCl₆, WO₂Cl₂, and (C₆H₅)₃PO were obtained from Alfa Products and used without further purification. 8-Hydroxyquinoline, 8-aminoquinoline, and (C₂H₅)₃N were purchased from Eastman and α,α' -bipyridyl and *o*-phenanthroline from Aldrich Chemicals. All solvents were distilled and dried by standard methods before use.

Syntheses. C₉H₇NS-HCl (8-mercaptoquinoline hydrochloride) was synthesized according to the method of Kealy and Freiser.¹⁴

WOC₃(THF)₂ was prepared by the method of Fowles and Frost.¹⁵ [(CH₃)₄N]₂[WOC₃] was prepared according to the procedure described by Allen et al.¹⁶ with the use of [(CH₃)₄N]Cl in place of the trialkylamine hydrochloride.

WOC₃(bpy) (green) was prepared by the method of Hull and Stiddard.¹⁷

WOC₃(bpy) (purple) was prepared by slow addition of 0.0064 mol of WOC₃(THF)₂ in 25.0 mL of dry, deaerated CH₂Cl₂ to a solution of 0.0064 mol of α,α' -bipyridyl in 25.0 mL of dry, deaerated CH₂Cl₂ under N₂. The solution was stirred for 30 min and filtered with use of Schlenk apparatus, and the purple precipitate was washed with two 10.0-mL portions of pentane and dried in vacuo. Anal. Calcd for WOC₃(C₁₀H₈N₂): C, 25.98; H, 1.74; N, 6.06; Cl, 23.00. Found: C, 25.75; H, 1.96; N, 5.94; Cl, 22.80. λ_{\max} (nm): 720 (2.25), 650 (2.24), 486 (2.64), 426 (2.71) (DMF, 0.1 M (C₂H₅)₄NCl; values in parentheses = log ϵ).

WOC₃(phen) was prepared in the same manner as described for WOC₃(bpy) above, giving a purple compound. Anal. Calcd for WOC₃(C₁₂H₈N₂): C, 29.63; H, 1.66; N, 5.76; Cl, 21.87. Found: C, 29.67; H, 1.94; N, 5.52; Cl, 21.33. λ_{\max} (nm): 746 (2.72), 400 (2.34) (DMF, 0.1 M (C₂H₅)₄NCl).

WOCl(ox)₂ was prepared by addition of a filtered solution of 0.0010 mol of [(CH₃)₄N]₂[WOC₃] in 40.0 mL of dry, deaerated C₂H₅OH to 40.0 mL of a solution containing 0.0035 mol of 8-hydroxyquinoline in dry, deaerated C₂H₅OH under N₂. After 10 min of stirring, 40.0 mL of freshly distilled, deaerated CH₃CN was slowly added and the solution stirred for 30 min. After cooling in an ice bath for 1 h, the solution was filtered, and the dark green precipitate was collected, washed with three 10.0-mL portions of pentane, and dried in vacuo. Anal. Calcd for WOCl(C₉H₆NO)₂: C, 41.29; H, 2.31; N, 5.35; Cl, 6.77. Found: C, 41.54; H, 2.44; N, 5.50; Cl, 6.73. λ_{\max} (nm): 651 (2.40), 461 (2.48) (DMF, 0.1 M (C₂H₅)₄NCl).

WOCl(tox)₂ was prepared by adding 0.0025 mol of 8-mercaptoquinoline hydrochloride in 50.0 mL of dry, deaerated CH₃CN to a filtered solution of 0.0015 mol of [(CH₃)₄N]₂[WOC₃] in dry, deaerated 50/50 by volume C₂H₅OH:CH₃CN under N₂. After 1 h of stirring, the solution was cooled in an ice bath for 1 h and filtered, and the dark wine precipitate was collected, washed once with 2.0 mL of C₂H₅OH, once with 2.0 mL of CH₃CN and twice with 10.0 mL of anhydrous diethyl ether, and dried in vacuo. Anal. Calcd for WOCl(C₉H₆NS)₂: C, 38.90; H, 2.18; N, 5.04; Cl, 6.38; S, 11.54. Found: C, 38.41; H, 2.37; N, 5.15; Cl, 5.98; S, 11.17. λ_{\max} (nm): 543 (2.47), 494 (3.00), 392 (3.70) (DMF, 0.1 M (C₂H₅)₄NCl). This complex is unstable toward oxygen and must be stored under vacuum.

WO₂Cl₂(OP(C₆H₅)₃)₂ and WO₂Cl₂(phen) were prepared by the method of Brisdon.¹⁸

WO₂Cl₂(bpy) and WO₂Br₂(bpy) were prepared by using the procedure of Hull and Stiddard.¹⁷

WO₂(ox)₂ was prepared by addition of 0.0040 mol of 8-hydroxyquinoline and 0.0040 mol of (C₂H₅)₃N in 50 mL of CH₃CN to a slurry of 0.0020 mol of WO₂Cl₂(OP(C₆H₅)₃)₂ in 50 mL of CH₃CN. The solution was stirred under reflux for 10 min and, after cooling in an ice bath for 30 min, yielded a yellow precipitate. The precipitate was collected, rinsed three times with 10.0-mL portions of anhydrous diethyl ether, and dried in vacuo. Anal. Calcd for WO₂(C₉H₆NO)₂: C, 42.88; H, 2.40; N, 5.56. Found: C, 43.17; H, 2.60; N, 5.58. λ_{\max} (nm): 356 (3.80), 311 (3.60) (DMF).

WO₂(tox)₂ was prepared by refluxing 0.0035 mol of 8-mercaptoquinoline hydrochloride, 0.0070 mol of (C₂H₅)₃N, and 0.0017 mol of WO₂Cl₂(OP(C₆H₅)₃)₂ for 10 min in 50.0 mL of dry C₂H₅OH. The hot solution deposited a gold product, which was collected, washed with two 10.0-mL portions of anhydrous diethyl ether, and dried over P₂O₅. Anal. Calcd for WO₂(C₉H₆NS)₂: C, 40.31; H, 2.26; N, 5.22; S, 11.96. Found: C, 40.28; H, 2.36; N, 5.36; S, 12.00. λ_{\max} (nm): 388 (3.95), 330 (3.60) (DMF).

WO₂(acac)₂ was prepared by a modification of the method of Nikolovski.¹⁹ A solution of 0.0017 mol of WO₂Cl₂(OP(C₆H₅)₃)₂ and 15.0 mL of acetylacetone in 30.0 mL of dry benzene was refluxed for 24 h. The volume was reduced to one-half and the solution stored in the freezer for 24 h. A small amount of anhydrous diethyl ether was added and the pale yellow precipitate collected, washed with four 10.0-mL portions of diethyl ether, and dried over P₂O₅.

Methods. Electrochemical measurements were made with a three-electrode cyclic voltammetric system described previously.⁸ DMF and (C₂H₅)₄NCl were purified and dried for electrochemical use according to literature procedures.²⁰

(13) E. I. Stiefel, *Prog. Inorg. Chem.*, **22**, 1 (1977).

(14) K. Kealy and H. Freiser, *Talanta*, **13**, 1382 (1966).

(15) G. W. A. Fowles and J. L. Frost, *J. Chem. Soc. A*, 671 (1967).

(16) E. A. Allen, B. J. Brisdon, D. A. Edwards, G. W. A. Fowles, and R. G. Williams, *J. Chem. Soc. A*, 4649 (1963).

(17) C. G. Hull and M. H. B. Stiddard, *J. Chem. Soc. A*, 1633 (1966).

(18) B. J. Brisdon, *Inorg. Chem.*, **6**, 1791 (1967).

(19) A. Nikolovski, *Croat. Chem. Acta*, **40**, 143 (1968).

(20) D. T. Sawyer and J. L. Roberts, Jr., "Experimental Electrochemistry for Chemists", Wiley, New York, 1974.

EPR spectra were recorded on a Varian V-4510 or a Bruker B-ER420 instrument, and EPR parameters were evaluated as described.²¹ The complexes were determined to be $90 \pm 10\%$ EPR active by comparison of their EPR signals with the EPR signals from $\text{MoOCl}(\text{ox})_2$, which had been calibrated by double integration against the EPR signal from $\text{K}_3\text{Mo}(\text{CN})_6$. Samples were prepared under prepurified N_2 (99.997%), transferred to 3.0-mm i.d. tubes with the use of gas-tight syringes, and frozen immediately in liquid nitrogen for low-temperature spectra. For room-temperature spectra, samples were transferred to a flat cell that had been evacuated and flushed with N_2 and kept under argon until spectra were recorded. Generally,

(21) A. Marchesini and P. M. H. Kroneck, *Eur. J. Biochem.*, **101**, 65 (1979).

$0.1 \text{ M } (\text{C}_2\text{H}_5)_4\text{NCl}$ was added to the solutions of the W(V) complexes, approximately $5.00 \times 10^{-4} \text{ M}$ in DMF, for stabilization.

Infrared spectra were recorded on a Beckman IR 20 instrument with the use of Nujol mulls.

Acknowledgment. This work was supported by Grant No. GM-08347 from the National Institutes of Health.

Registry No. *cis*- $\text{WOC}l_3(\text{bpy})$, 77340-55-7; *trans*- $\text{WOC}l_3(\text{bpy})$, 77285-89-3; *trans*- $\text{WOC}l_3(\text{phen})$, 77224-45-4; *cis*- $\text{WOC}l(\text{ox})_2$, 77224-46-5; *cis*- $\text{WOC}l(\text{tox})_2$, 77224-47-6; $\text{WO}_2\text{Cl}_2(\text{bpy})$, 18252-71-6; $\text{WO}_2\text{Cl}_2(\text{phen})$, 18252-72-7; $\text{WO}_2(\text{ox})_2$, 21289-71-4; $\text{WO}_2(\text{tox})_2$, 55835-57-9; $\text{WO}_2\text{Br}_2(\text{bpy})$, 12116-32-4; $\text{WO}_2(\text{acac})_2$, 21292-49-9; $\text{WOC}l_3(\text{THF})_2$, 18131-65-2; $[(\text{CH}_3)_4\text{N}]_2[\text{WOC}l_5]$, 77224-48-7; $\text{WO}_2\text{Cl}_2(\text{OP}(\text{C}_6\text{H}_5)_3)_2$, 18252-68-1.

Contribution from the Departments of Chemistry, Abilene Christian University, Abilene, Texas 79699, and Texas A&M University, College Station, Texas 77843, and from the Exxon Research and Engineering Company, Florham Park, New Jersey 07932

Iron–Sulfur Stretching Band Assignments in High-, Low-, and Mixed-Spin Iron(III) Dialkyldithiocarbamates

BENNETT HUTCHINSON,* PAUL NEILL, AL FINKELSTEIN,¹ and JAMES TAKEMOTO

Received October 6, 1980

The far-infrared spectra of several iron(III) dialkyldithiocarbamates having room-temperature magnetic moments in the high-, low- and intermediate-spin range have been reinvestigated. Iron–sulfur stretching vibrations have been assigned with the use of ^{54}Fe and ^{56}Fe isotopes. The high-spin Fe–S stretching vibrations appear at $205\text{--}250 \text{ cm}^{-1}$ and the low spin at $305\text{--}350 \text{ cm}^{-1}$, and the intermediate spin show Fe–S stretching bands in both regions. Results of spectral measurements above and below room temperature are explained on the basis of these assignments.

Introduction

The ability of dialkyldithiocarbamate (R_2dtc) ligands to stabilize iron(III) in high-spin, low-spin, and “intermediate”-spin magnetic moment arrangements has been recognized and investigated with the use of a variety of methods.^{2–14} In the far-infrared spectral region, vibrational spectroscopy has been employed because metal–ligand stretching bands which appear in this region may provide information about the strength of the metal–ligand bonds and the symmetry of the molecule. Such data are also used in calculating the value of the partition function,⁷ estimating a value for the entropy of the systems,¹⁵ and distinguishing between models of the “intermediate” spin systems.⁸ For this information to be useful, the metal–ligand stretching bands should be correctly assigned. Although some progress has been realized in the assignment of the Fe–S stretching bands for

Table I. Previous $\nu(\text{Fe-S})$ Assignments in $\text{Fe}(\text{R}_2\text{dtc})_3$

compd	high-spin	low-spin	ref
$\text{Fe}[(\text{pyr})\text{dtc}]_3$	328		8
$\text{Fe}[(\text{pyr})\text{dtc}]_3$	320		5
$\text{Fe}[(\text{pyr})\text{dtc}]_3$	334, 324 ^a		7
$\text{Fe}(i\text{-Pr}_2\text{dtc})_3$		365, 320	5
$\text{Fe}(N,N\text{-c-Hx}_2\text{dtc})_3$		346	8
$\text{Fe}(\text{Me}_2\text{dtc})_3$	360	334, 305	7
$\text{Fe}(N\text{-Et-N-Phdtc})_3$	304 ^b	341 ^b	8
$\text{Fe}(\text{Et}_2\text{dtc})_3$	355	552	14
$\text{Fe}(\text{Pr}_2\text{dtc})_3$	307	367	7

^a Measured at 30 K. ^b Assigned on the basis of $^{54}\text{Fe}/^{56}\text{Fe}$.

these iron(III) complexes, conflicting assignments remain unresolved in several instances. The appearance of ligand absorptions in the same region as the Fe–S stretching bands have made assignments more difficult.

Presently there are four principal investigations in the literature which discuss the Fe–S stretching band assignments in these complexes. These assignments are summarized in Table I. Ewald et al. proposed the $300\text{--}400\text{-cm}^{-1}$ region for both high- and low-spin Fe–S stretching bands from their study of five $\text{Fe}(\text{R}_2\text{dtc})_3$ complexes at room and liquid air temperatures.⁵ Hall and Hendrickson extended the previous study by investigating a larger number of $\text{Fe}(\text{R}_2\text{dtc})_3$ complexes plus related compounds and improving the resolution at lower temperatures.⁷ They also assigned all Fe–S stretching bands in the $300\text{--}400\text{-cm}^{-1}$ region, placing the high-spin Fe–S stretching modes at higher energy than the low-spin Fe–S stretching modes. Butcher, Ferraro, and Sinn examined the far-infrared spectra of four $\text{Fe}(\text{R}_2\text{dtc})_3$ complexes using variable pressures and employing $^{54}\text{Fe}\text{--}^{56}\text{Fe}$ isotopic substitution for one, $\text{Fe}(N\text{-Et-N-Phdtc})_3$.⁸ These authors assigned the high-spin Fe–S stretch at lower energy than the low-spin Fe–S stretching modes but kept both in the $300\text{--}400\text{-cm}^{-1}$ region. More recently, Sorai studied the variable-temperature far-infrared spectra of $\text{Fe}(\text{Et}_2\text{dtc})_3$ and assigned the low-spin Fe–S

* To whom correspondence should be addressed at Abilene Christian University.

- (1) Taken in part from: A. Finkelstein, Thesis, Texas A&M, 1973.
- (2) (a) A. H. Ewald, R. L. Martin, I. G. Ross, and A. H. White, *Proc. R. Soc. London, Ser. A*, **A280**, 235 (1964); (b) R. M. Golding and H. J. Whitfield, *Trans. Faraday Soc.*, **62**, 1713 (1966).
- (3) E. Frank and C. R. Abeledo, *Inorg. Chem.*, **5**, 1453 (1966).
- (4) R. Richards, C. E. Johnson and H. A. O Hill, *J. Chem. Phys.*, **48**, 532 (1968).
- (5) A. H. Ewald, R. L. Martin, E. Sinn and A. H. White, *Inorg. Chem.*, **8**, 1837 (1969).
- (6) M. J. Tricker, *J. Inorg. Nucl. Chem.*, **36**, 1543 (1974).
- (7) G. R. Hall and D. N. Hendrickson, *Inorg. Chem.*, **15**, 2077 (1976).
- (8) R. J. Butcher, J. R. Ferraro and E. Sinn, *Inorg. Chem.*, **15**, 2077 (1976).
- (9) J. M. de Lisle and R. M. Golding, *Proc. R. Soc. London, Ser. A*, **A296**, 457 (1967).
- (10) P. B. Merrithew and P. G. Rasmussen, *Inorg. Chem.*, **11**, 325 (1972).
- (11) P. C. Healy and A. H. White, *J. Chem. Soc., Dalton Trans.*, 1163 (1972).
- (12) J. G. Leopoldt and P. Coppens, *Inorg. Chem.*, **12**, 2269 (1973).
- (13) A. H. White, R. Roper, E. Kokot, H. Waterman and R. L. Martin, *Aust. J. Chem.*, **17**, 294 (1964).
- (14) M. Sorai, *J. Inorg. Nucl. Chem.*, **40**, 1031 (1978).
- (15) J. Fleisch, P. Gülich, and K. M. Hasselbach, *Inorg. Chem.*, **16**, 1979 (1977).